Global analysis of phosphorylation and ubiquitylation cross-talk in protein degradation

Danielle L Swaney[1], Pedro Beltrao[2], Lea Starita[1,3], Ailan Guo[4], John Rush[4], Stanley Fields[1,3,5], Nevan J Krogan[6,7] & Judit Villén[1]

Cross-talk between different types of post-translational modifications on the same protein molecule adds specificity and combinatorial logic to signal processing, but it has not been characterized on a large-scale basis. We developed two methods to identify protein isoforms that are both phosphorylated and ubiquitylated in the yeast *Saccharomyces cerevisiae*, identifying 466 proteins with 2,100 phosphorylation sites co-occurring with 2,189 ubiquitylation sites. We applied these methods quantitatively to identify phosphorylation sites that regulate protein degradation via the ubiquitin-proteasome system. Our results demonstrate that distinct phosphorylation sites are often used in conjunction with ubiquitylation and that these sites are more highly conserved than the entire set of phosphorylation sites. Finally, we investigated how the phosphorylation machinery can be regulated by ubiquitylation. We found evidence for novel regulatory mechanisms of kinases and 14-3-3 scaffold proteins via proteasome-independent ubiquitylation.

Protein post-translational modifications (PTMs) function as highly versatile switches that regulate protein activity, concentration and subcellular localization and that maintain homeostasis. One or more residues in a protein can be modified, either in an independent fashion or combinatorially, to confer specific protein regulation[1,2]. However, both the basis and prevalence of PTM cross-talk, in which the presence of one modification influences the appearance of others, remain unknown.

Two of the most prevalent PTMs in eukaryotic proteomes, phosphorylation and ubiquitylation, are integral to almost every cellular process. Phosphorylation is the primary mechanism for regulating cellular signaling, whereas ubiquitylation plays a prominent role in protein degradation. Cross-regulation between phosphorylation and ubiquitylation can take many forms[2]. PTMs can regulate the machinery of other modification types, such as the activation of E3 ubiquitin ligase activity by phosphorylation[3–5]. The coordinated targeting of a substrate by multiple modification types provides another example of cross-talk. This is perhaps best exemplified by phosphodegrons, in which one or more phosphorylation sites function in a *cis*-regulatory manner to promote the subsequent ubiquitylation of a substrate. Phosphodegrons are critical to cell-cycle progression, to which they impart irreversibility and robustness. Given the evidence for co-regulation between phosphorylation and ubiquitylation, and the influence of these PTMs on a wide variety of cellular processes, we set out to characterize the scope of cross-talk between these two modifications.

Proteomics based on mass spectrometry has emerged as a powerful tool to characterize protein modifications and has demonstrated that thousands of proteins are post-translationally modified at any given time[5–9]. To date, most studies have focused on a single type of modification in isolation owing to two limitations[10–12]. First, modifications often exist at substoichiometric levels and require highly specific enrichment methods. Second, proteomics is most commonly performed on peptides rather than on intact proteins, and such experiments often sever the connection between multiple modifications present on a single protein isoform. With these limitations in mind, we developed two enrichment strategies that permit the global identification of comodified proteins and applied these methods to investigate ubiquitylation-phosphorylation cross-talk in the context of protein degradation. Using these approaches, we found that distinct phosphorylation sites often co-occur with ubiquitylation, and we identified several new phosphodegrons.

RESULTS

Development of methods to identify comodified proteins

To probe combinatorial PTM cross-talk, we developed two methods to enrich for proteins containing two PTM types. The specific enrichment approaches developed here are targeted at the evaluation of ubiquitylation and phosphorylation cross-talk but should be generally applicable to many PTM types.

In the first enrichment approach, we applied cobalt-NTA (nitrilotriacetic acid) affinity purification to enrich for proteins modified with His-tagged ubiquitin during log-phase growth in

[1]Department of Genome Sciences, University of Washington, Seattle, Washington, USA. [2]European Molecular Biology Laboratory–European Bioinformatics Institute, Wellcome Trust Genome Campus, Hinxton, UK. [3]Howard Hughes Medical Institute, University of Washington, Seattle, Washington, USA. [4]Cell Signaling Technology Inc., Danvers, Massachusetts, USA. [5]Department of Medicine, University of Washington, Seattle, Washington, USA. [6]Department of Cellular and Molecular Pharmacology, University of California, San Francisco, San Francisco, California, USA. [7]California Institute for Quantitative Biosciences (QB3), San Francisco, California, USA. Correspondence should be addressed to J.V. (jvillen@u.washington.edu).

RECEIVED 31 JULY 2012; ACCEPTED 2 MAY 2013; PUBLISHED ONLINE 9 JUNE 2013; DOI:10.1038/NMETH.2519

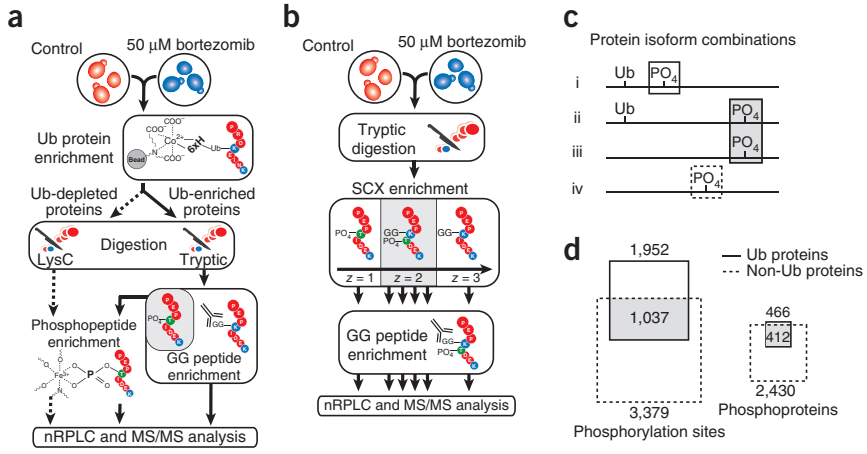

Figure 1 | Overview of methodology and PTMs identified. We used two enrichment strategies (illustrated here in the context of the proteasome inhibition experiment). (**a**) In the first enrichment method, samples were enriched for ubiquitylated (Ub) proteins with affinity purification of His-tagged ubiquitin. Nonubiquitylated (Non-Ub) proteins (dotted lines) were digested with LysC and enriched for phosphopeptides. Ub proteins (solid lines) were digested with trypsin and further enriched for diGly peptides and for phosphopeptides, which was followed by mass spectrometry analysis. (**b**) In the second enrichment method, proteins were digested with trypsin into peptides and enriched for doubly charged peptides via strong-cation exchange (SCX). All SCX fractions were further enriched for diGly peptides before mass spectrometry analysis. (**c**) Four cases showing how the same protein can exist in different combinations of modification states: a phosphorylation site unique to the ubiquitylated protein isoform (**i**), phosphorylation sites found in both ubiquitylated (**ii**) and nonubiquitylated (**iii**) isoforms, and a phosphorylation site unique to nonubiquitylated protein isoforms (**iv**). (**d**) Overlap of non-Ub and Ub samples with respect to phosphorylation sites and phosphoproteins. *z*, charge state. nRPLC, nano–reversed-phase liquid chromatography.

S. cerevisiae[13] (**Fig. 1a**). This ubiquitin-enriched population we refer to as ubiquitylated proteins, whereas the ubiquitin-depleted flow-through we refer to as nonubiquitylated proteins (**Supplementary Fig. 1**). After carrying out tryptic digestion, we enriched for phosphopeptides in both the ubiquitin-enriched population and the flow-through. Additionally, to identify individual ubiquitylation sites in the ubiquitin-enriched population, we used an antibody to enrich for peptides with the characteristic glycine-glycine (diGly) remnant that remains on ubiquitylated lysine residues after tryptic digestion. We analyzed the three samples (nonubiquitylated phosphopeptides, ubiquitylated phosphopeptides and ubiquitylated nonphosphopeptides) with nano–reversed-phase liquid chromatography (nRPLC) coupled to tandem mass spectrometry (MS/MS). The quantities of PTM sites and protein identifications are listed in **Table 1**.

Though this first method permits identification of proteins modified by both ubiquitylation and phosphorylation regardless of the proximity of these modifications on the protein sequence, it cannot establish which two sites are present on the same isoform. Thus, we developed a second approach to directly identify peptides concurrently modified by phosphorylation and ubiquitylation.

The second approach relies on sequential peptide-based enrichment to identify peptides containing multiple PTM types. With this method, one can establish that both PTMs are present on the same protein isoform, but this approach is limited to identifying PTM sites found in close sequence proximity. We used strong cation–exchange (SCX) chromatography to first separate tryptic peptides by their solution charge (**Fig. 1b**). SCX has previously been applied to enrich for PTMs that alter solution charge state, and we show here that it can also be used to enrich for both ubiquitylated peptides and ubiquitylated phosphopeptides[14,15] (**Supplementary Fig. 2a**). Ubiquitylated peptides represent a substoichiometric population; thus, each SCX fraction was further enriched for the diGly ubiquitin remnant with an antibody, and all fractions were analyzed by nRPLC coupled to MS/MS. This second method resulted in 1,008 unique identifications of ubiquitylated phosphopeptides as compared to only 56 with the first method (**Supplementary Fig. 2b**, **Table 1** and **Supplementary Data 1**).

A total of 466 proteins comodified with ubiquitylation and phosphorylation were identified in these qualitative experiments (**Table 1** and **Fig. 1c**, **i**,**ii**). Nearly all ubiquitylated phosphoproteins were also identified in a nonubiquitylated phosphoprotein isoform (**Fig. 1c**, **iii**, **d**). However, a smaller degree of overlap was observed at the phosphorylation-site level (**Fig. 1c**, **iv**, **d**). These results suggest that protein isoforms modified with ubiquitin carry unique phosphorylation sites that likely distinguish their specific function relative to that of their nonubiquitylated isoforms. We also compared the Gene Ontology enrichment of ubiquitylated phosphoproteins and nonubiquitylated phosphoproteins. Ubiquitylated phosphoproteins were enriched for localization in the ribosome, membranes and cell bud and for processes such as protein translation and transmembrane transport (**Fig. 2a** and **Supplementary Table 1**). In agreement

Table 1 | Protein and PTM identifications from qualitative experiments

Group	Sample	Ubiquitylated proteins	Ubiquitylated phosphoproteins	Ubiquitylation sites	Phosphorylation sites
1	Ubiquitylated proteins from affinity-purification method	891	321	2,395	1,769
2	Ubiquitylated proteins from SCX-IP method	1,817	245	4,659	437
	Total ubiquitylated proteins	1,920	466	5,629	2,100
			Phosphoproteins		Phosphorylation sites
3	Nonubiquitylated proteins		2,376		11,704

SCX-IP, strong-cation exchange–immunoprecipitation.

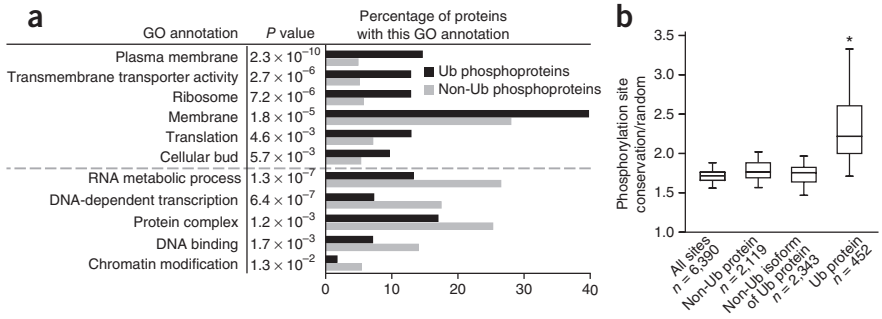

Figure 2 | Evolution and functional enrichment of modification sites. (**a**) Gene Ontology (GO) enrichment analysis of ubiquitylated (Ub) phosphoproteins and nonubiquitylated (non-Ub) phosphoproteins. GO enrichment was performed using Babelomics4. (**b**) For different populations of proteins, we calculated the fraction of conserved phosphorylation sites over conserved amino acids from random sampling of the same number of phospho-acceptor residues (Ser, Thr). Whiskers represent the lowest and highest data points within 1.5 times the interquartile range (*P = 0.0027, Kolmogorov-Smirnov test).

with these results, we found ubiquitylated phosphoproteins to be enriched for several transporter and arrestin domains (**Supplementary Table 2**).

Conservation and function of sites on comodified proteins

To study the evolutionary conservation of phosphorylation and ubiquitylation sites, we aligned yeast proteins with their respective human orthologs. A PTM was defined as conserved when the yeast protein and the human protein were modified in the same region of the alignment. We found ubiquitylation sites in yeast to be more conserved than expected by random chance. However, the level of conservation was not specific to the absence or presence of phosphorylation. Ubiquitylation sites on phosphoproteins had a similar level of conservation over random expectation with respect to all ubiquitylation sites (P = 0.26, Kolmogorov-Smirnov test; **Supplementary Fig. 3**).

We next examined the conservation of phosphorylation sites (**Fig. 2b**). We compared the conservation over random of four groups of yeast phosphorylation sites: all phosphorylation sites, phosphorylation sites on nonubiquitylated protein isoforms (**Fig. 1c**, **iv**), phosphorylation sites on ubiquitylated proteins but identified in nonubiquitylated isoforms (**Fig. 1c**, **iii**), and phosphorylation sites found co-occurring with ubiquitylation (**Fig. 1c**, **i**,**ii**). We observed that phosphorylation sites found co-occurring with ubiquitylation were more conserved (over random expectation) than were all other phosphorylation site groups tested (P = 0.0027, Kolmogorov-Smirnov test). This result suggests that phosphorylation sites found co-occurring with protein ubiquitylation are more likely to be functionally important[16,17].

Characterization of the response to proteasome inhibition

After developing methodologies to identify proteins comodified with phosphorylation and ubiquitylation, we sought to globally investigate the relationship between phosphorylation and ubiquitylation in the context of proteasome-mediated degradation. The proteasome is responsible for the degradation of ubiquitylated proteins. It functions globally to modulate protein concentrations and remove misfolded or damaged proteins. It also promotes cell-cycle progression by degrading specific proteins at precise phase transitions of the cell division cycle[18–21]. Certain proteasome substrates are known to require the presence of specific phosphorylation sites, known as phosphodegrons, to direct ubiquitylation and proteasome-mediated degradation.

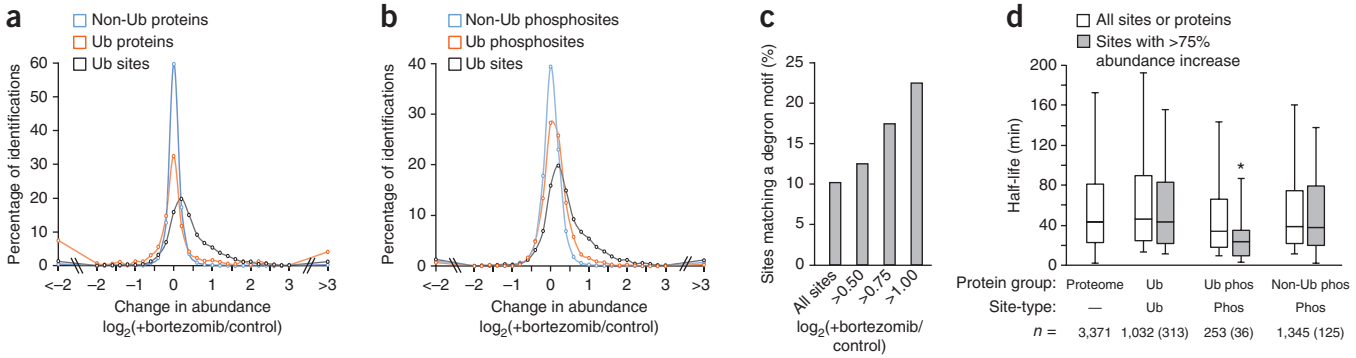

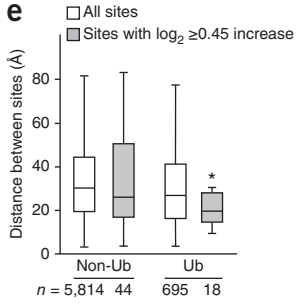

Figure 3 | The effect of proteasome inhibition on protein and PTM site abundance, and properties of regulated phosphorylation sites. (**a**) $\log_2$ distributions of abundance changes for proteins and ubiquitylation sites in response to proteasome inhibition (by application of 50 μM bortezomib for 1 h). (**b**) $\log_2$ distributions of abundance changes for phosphorylation and ubiquitylation sites. (**c**) Distribution of sites matching a phosphodegron motif at various intervals of abundance changes after proteasome inhibition. (**d**) Half-life distributions for all protein identifications compared to those for proteins containing sites increasing in abundance by >75% (*$P = 6.3 \times 10^{-3}$); whiskers represent the 10th and 90th percentiles. Protein half-life values were obtained from the literature[22]. (**e**) Pairwise spatial distance (angstroms between α carbons) either between phosphorylation sites co-occurring with lysine ubiquitylation sites (Ub) or between the position of these same ubiquitylation sites and phosphorylation sites identified on nonubiquitylated isoforms (Non-Ub). Distances between all pairs (white) are compared to the distances between pairs for which both sites increase in abundance upon proteasome inhibition (gray) (*P < 0.0043). Whiskers represent the lowest and highest data points within 1.5 times the interquartile range.

Table 2 | Quantifications from proteasome inhibition experiments (SILAC)

Group	Sample	Ubiquitylated proteins	Ubiquitylated phosphoproteins	Ubiquitylated isoforms	Phosphorylated isoforms
1	Ubiquitylated proteins from affinity-purification method	558 (62)	322	3,816 (628)	1,710 (54)
2	Ubiquitylated proteins from SCX-IP method	1,176	108	2,787 (119)	303 (10)
	Total ubiquitylated proteins	1,307	378	5,465	2,048
		Proteins	Phosphoproteins		Phosphorylated isoforms
3	Nonubiquitylated proteins	3,484 (28)	1,939	N/A	10,656 (159)

Values in parentheses indicate the number of proteins or isoforms increasing in abundance by greater than twofold. SCX-IP, strong-cation exchange–immunoprecipitation; SILAC, stable-isotope labeling by amino acids in cell culture.

We measured the quantitative changes in proteins, phosphorylation sites and ubiquitylation sites upon proteasome inhibition with bortezomib by performing a stable-isotope labeling by amino acids in cell culture (SILAC) experiment (**Fig. 3a**,**b**, **Table 2** and **Supplementary Data 1**). We analyzed both ubiquitylated and nonubiquitylated protein samples (**Fig. 1a**,**b**) via mass spectrometry before phosphopeptide and diGly remnant enrichment to assess quantitative changes at the protein level; the distribution of protein abundances was mostly unaffected by proteasome inhibition (**Fig. 3a**). Protein changes were mostly observed in the ubiquitylated population, in which an abundance fold increase of >2 was observed for 11.1% of proteins, whereas <1% of nonubiquitylated protein increased by more than twofold (**Fig. 3a** and **Table 2**). Overall, increases in protein abundances among ubiquitylated isoforms did not cause depletions of these proteins from the nonubiquitylated pool. This result supports the hypothesis that ubiquitylated protein isoforms represent a small fraction of the total pool of a given protein[6].

Proteasome inhibition caused an increase in the median abundance of ubiquitylated peptides, with 12.9% of ubiquitylated peptide isoforms increasing in abundance by more than twofold, whereas phosphorylation sites on ubiquitylated proteins were affected to a lesser extent: 3.4% increased by more than twofold (**Fig. 3b** and **Table 2**). Increases in ubiquitylation-site abundance were not correlated with increases in protein abundance. Only 13.4% of proteins with an increase in ubiquitylation sites of more than twofold also displayed a similar increase in protein abundance. This suggests that proteasome inhibition increases the stoichiometry of ubiquitylation sites on already ubiquitylated proteins rather than promoting ubiquitin conjugation to previously nonubiquitylated protein molecules. As further evidence, we found that proteins containing a site of ubiquitylation doubling in abundance were half as likely to be represented by a single isoform as compared to all ubiquitylated proteins (20.2% versus 40.5%, $P = 4.4 \times 10^{-12}$). Thus, the majority of ubiquitylated proteins contained multiple isoforms that could be differentially regulated upon proteasome inhibition.

Properties of regulated phosphorylation sites

We expected that upon proteasome inhibition, phosphorylation sites within phosphodegrons would increase in abundance. We found that phosphorylation sites on ubiquitylated proteins that increased in abundance were indeed more likely to match a degron motif (**Fig. 3c**). The increase in abundance of a phosphorylation site often corresponded to an increase in ubiquitylation-site abundance (**Supplementary Fig. 4a**); however, the presence of a degron motif was not sufficient to predict ubiquitylation-site abundance changes (**Supplementary Fig. 4b**). These results suggest that measuring the response to proteasome inhibition of both phosphorylation sites and ubiquitylation sites is important for identifying phosphodegrons.

Many canonical phosphodegrons are found in short-lived cell-cycle proteins. Thus, we analyzed the distribution of half-lives for ubiquitylated proteins, ubiquitylated phosphoproteins and nonubiquitylated phosphoproteins[22] (**Fig. 3d**). We compared the distribution of the whole group and the subset of proteins from each group that contained a site increasing in abundance by >75%. We found that the ubiquitylated phosphoproteins with a phosphorylation site increasing in abundance had significantly shorter half-lives ($P = 6.3 \times 10^{-3}$), whereas sites increasing in abundance in other protein groups were not significantly different. Functional enrichment analysis of this population revealed that 30% could be classified as either cell-cycle or cell-division proteins ($P = 0.02$). These results reinforce the role of phosphodegrons in the regulation of cell-cycle proteins, but they also show that the degradation of proteins with alternative functional roles is also regulated by phosphodegrons.

We hypothesized that cross-talk between phosphorylation and ubiquitylation would be found in pairs of modification sites in close proximity. To study this, we mapped modification sites onto protein structure homology models of yeast proteins. We calculated the spatial distance either between phosphorylation sites and their co-occurring lysine ubiquitylation sites (**Fig. 1c**, **i**,**ii**) or between the position of these same ubiquitylation sites and phosphorylation sites identified on nonubiquitylated isoforms (**Fig. 1c**, **iv**). Phosphorylation sites co-occurring with ubiquitylation showed a small but highly significant decrease in distance to ubiquitylation sites when compared to other phosphorylation sites ($P = 3.1 \times 10^{-9}$; **Fig. 3e**). Phosphorylation-ubiquitylation pairs that were co-regulated in abundance and increased together upon proteasome inhibition were significantly closer than were other pairs ($P = 0.0043$). We did not observe this result with regulated phosphorylation sites not co-occurring with ubiquitylation (**Fig. 3e**). Together these results suggest that the molecular mechanisms that mediate the cross-talk between these two modifications impose spatial constraints and that the pairs of sites identified by our method have mechanistic implications.

Co-regulation of phosphorylation and ubiquitylation sites

The current literature contains a collection of phosphodegrons that have been identified through targeted biochemical assays. To identify novel potential phosphodegrons, we considered ubiquitylation- and phosphorylation-site pairs that displayed correlated accumulation upon proteasome inhibition. We identified a total of 180 ubiquitin- and phosphorylation-site pairs in which both modifications increased in abundance (**Supplementary Data 2**). These pairs included several proteins with known phosphodegron

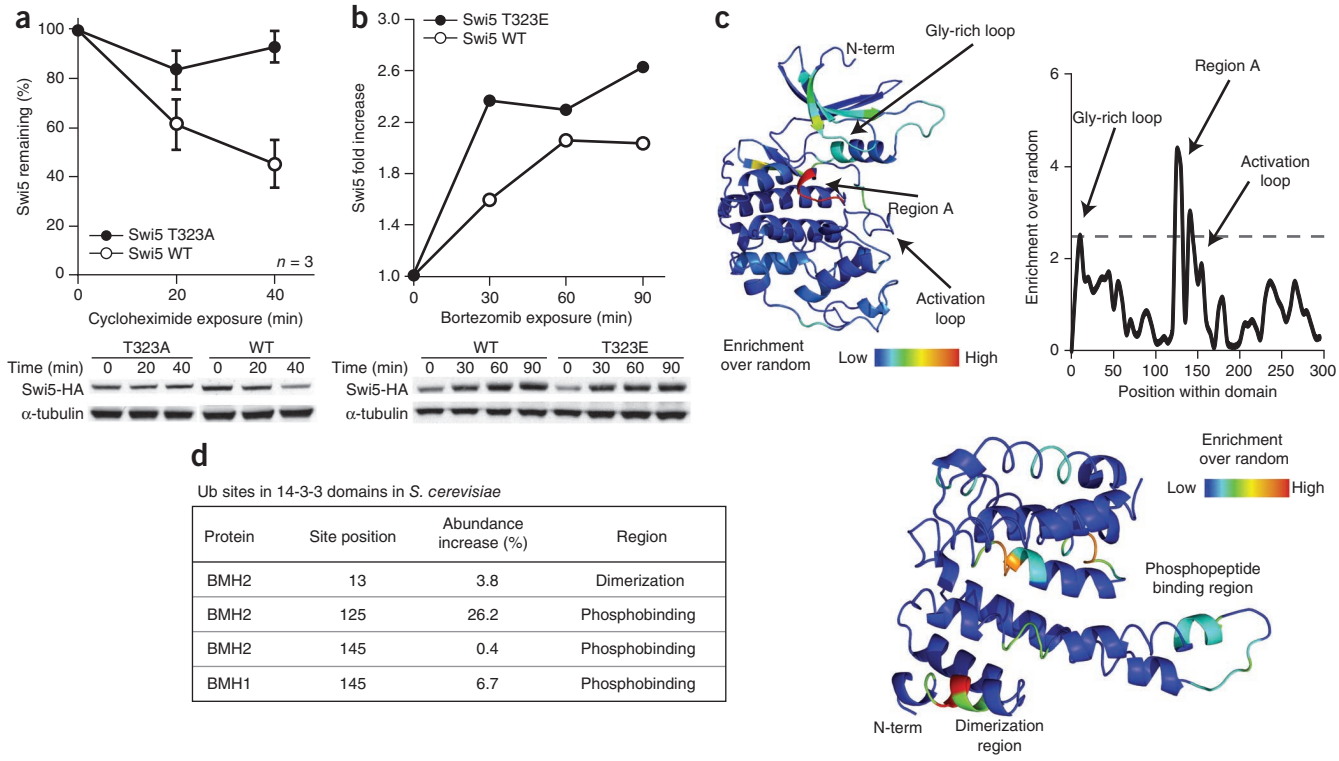

Protein	Site position	Abundance increase (%)	Region
BMH2	13	3.8	Dimerization
BMH2	125	26.2	Phosphobinding
BMH2	145	0.4	Phosphobinding
BMH1	145	6.7	Phosphobinding

Figure 4 | Validation of a new phosphodegron and ubiquitin–mediated regulation of phosphorylation machinery. (**a**,**b**) Yeast cells were treated with galactose to induce Swi5 expression and incubated with either cycloheximide to measure protein degradation ($n = 3$) (**a**) or bortezomib to measure protein accumulation (**b**). Aliquots were taken at the indicated times, and protein expression was monitored by immunoblotting with anti-hemagglutinin (anti-HA) to detect Swi5 or anti–α-tubulin for a loading control. Degradation levels measured from immunoblotting were quantified in triplicate, and bortezomib-induced accumulation was quantified from a single replicate. (**c**) Enrichment of ubiquitylation sites in the structure of the kinase domain. A representative structure pertaining to Protein Data Bank (PDB) ID 1QMZ is shown. Right, the graph represents the numeric values of enrichment over random for different positions within the kinase domain. Relevant regions within the domain are indicated. (**d**) Enrichment of ubiquitylation sites within the 14-3-3 phosphorylation-binding domain (PDB ID 3MHR). The table lists ubiquitylation sites identified in the phosphobinding and dimerization regions of the two 14-3-3 domain–containing proteins in *S. cerevisiae* and the percent increase in abundance upon proteasome inhibition measured in this study.

sites (such as Ash1, Far1 and Ho) but in many cases represented different phosphorylation sites than previously reported[20,23,24]. In some instances, however, phosphodegrons are composed of multiple phosphorylation sites, and different combinations of sites on the same protein can stimulate protein degradation[18]. Therefore, these new sites on previously identified phosphodegron-containing proteins may contribute to the previously observed effects or may represent alternative degradation signals.

To further validate our approach, we tested the impact of a specific phosphorylation site on protein degradation via a complementary methodology. In the present work, we identified the protein Swi5 as containing one phosphorylation site (Thr323) and three ubiquitylation sites in this region (Lys227, Lys270 and Lys315), all increasing in abundance upon proteasome inhibition. In yeast, Swi5 regulates the transcription of *SIC1*, and during early G1 phase, Swi5 is targeted for degradation via the SCF^{Cdc4} complex[25]. In previous work, eight potential Cdk target sites (Ser225, Ser231, Ser246, Ser250, Ser261, Ser300, Thr320 and Thr323) were simultaneously mutated to alanine, which increased protein stability and delayed entry into S phase[25,26]. We tested the candidate phosphodegron site identified in our study, Swi5 Thr323, by generating a yeast strain carrying a T323A mutation. The degradation of the mutant was compared to that of the wild-type protein. The T323A mutation stabilized the protein relative to the wild type (**Fig. 4a** and **Supplementary Fig. 5a**,**b**). We also generated a strain containing a T323E mutation to mimic a permanently phosphorylated state. Upon proteasome inhibition, this mutant accumulated at a faster rate and to a greater extent than wild-type Swi5 (**Fig. 4b**). These results demonstrate that Swi5 Thr323 phosphorylation is a phosphodegron site and validate the ability of our approach to identify functional PTM cross-talk.

We evaluated an additional phosphorylation site that represents the diversity in function of phosphodegrons. We observed a single site of ubiquitylation (Lys329) on the GTPase Gic2 and numerous phosphorylation sites, all increasing in abundance upon proteasome inhibition. Previous work has demonstrated that phosphorylation of Gic2 Ser254 and/or Ser258 serves as a phosphodegron; mutations to alanine inhibit, but do not block, Gic2 degradation[27]. Here we mutated an alternative potential phosphodegron site, Gic2 S360A. This inhibited but did not block Gic2 degradation, whereas the phosphomimetic Gic2 S360E mutant caused more rapid degradation of Gic2 relative to that of wild type (**Supplementary Fig. 5c**,**d**). In agreement with previous work, these results suggest that several phosphorylation sites contribute to the total phosphodegron signal on Gic2, much as in the well-studied case of Sic1.

Ubiquitylation regulates the phosphorylation machinery

We examined the potential for ubiquitylation to regulate the phosphorylation machinery by evaluating the enrichment (that is, the conservation) of ubiquitylation sites in protein kinases, phosphatases and phosphobinding domains, using previously described methods[12]. To obtain robust statistics, we included ubiquitylation sites found here along with sites from human and mouse studies[5–7]. We mapped these sites onto a representative structure of each domain family and performed statistical analysis to find regions that were commonly modified by ubiquitin. Within the protein kinase domain family, a total of 72 proteins showed enrichment of ubiquitylation sites either in the glycine-rich loop (30 of 388 sites) or in Region A, N-terminal to the activation loop (55 of 388 sites ($P < 0.005$); **Fig. 4c**).

Proteins of the 14-3-3 domain family bind phosphorylated targets. These proteins primarily function as dimers, with each monomer binding a different protein target or a different region of the same protein target[28]. Ubiquitylation sites in the 14-3-3 domains from 19 proteins from either human, mouse or the yeast *S. cerevisiae* were significantly enriched in two functionally important regions: the N-terminal helix (25 of 171 sites), required for dimerization, and a helix that forms the phosphopeptide binding pocket (60 of 171 sites ($P < 0.005$); **Fig. 4d**). The function of this ubiquitylation is independent of degradation, as ubiquitylation sites from the two 14-3-3 proteins in *S. cerevisiae*, Bmh1 and Bmh2, did not change upon proteasome inhibition (**Fig. 4d**).

No regions were significantly enriched for ubiquitylation within phosphatases or for phosphorylation sites among different types of the ubiquitylation machinery (data not shown).

DISCUSSION

Cross-talk between different protein PTMs is an emerging theme in biology, but thus far it has been observed only on histones and a few other proteins. The study of PTM cross-talk has been a major challenge because methods are lacking to determine whether two PTMs co-occur on the same protein. We have developed two methods to identify PTM cross-talk between any PTM pair on a proteome-wide basis. Our first approach relies on affinity-purification enrichment of proteins containing a specific PTM followed by subsequent enrichment of the other PTM type. This approach is best suited for applications of cross-talk in which one PTM type can be isolated at high purity. Our second approach, based on SCX fractionation, is applicable to the study of cross-talk between any PTMs in which one PTM changes the solution charge state, though the method can characterize only PTMs that are close in sequence proximity. When used in combination, however, these methods provide a more comprehensive view of PTM cross-talk, and we expect that these methods will find application in future studies of protein regulation by multiple PTM types.

A central question in PTM cross-talk is how one modification site regulates surrounding modification sites. In the case of phosphodegrons, phosphorylation promotes subsequent ubiquitylation. However, is this directionality globally true? We found greater conservation of phosphorylation on ubiquitylated proteins, a characteristic indicative of biological function[12,16,17]. The reverse analysis evaluating the conservation of ubiquitylation sites on phosphoproteins versus nonphosphorylated proteins revealed no differences. These results suggest a global cross-talk directionality, in which phosphorylation more frequently precedes ubiquitylation.

In addition to investigating PTM cross-talk, our work reveals new insights into the regulatory roles of ubiquitylation. To our surprise, many instances of increased ubiquitylation were not accompanied by corresponding changes in protein abundance. Instead, already ubiquitylated proteins became ubiquitylated on other residues, increasing the stoichiometry. One interpretation of these results is that ubiquitylation of these other residues serves as a distress signal for the cell to rapidly degrade that protein molecule. Alternatively, more complex signaling may be at play, in which specific ubiquitylation sites are used as degradation markers, whereas others serve to modulate protein function in a reversible fashion.

Besides the combinatorial PTM cross-talk found in comodified proteins, PTMs can alter the activity of proteins that regulate a different PTM. Kinases have a highly conserved kinase domain that can be regulated by phosphorylation. Phosphorylation of the activation loop causes activating structural changes, and phosphorylation of the glycine-rich region can regulate ATP binding[29]. The precise enrichment of ubiquitylation near the domain activation loop and in the glycine-rich region suggests an additional mode of kinase regulation by ubiquitylation: reversible inhibition. We hypothesize that the steric hindrance of a ubiquitin attachment in either of these regions serves as a rapid means to transiently inhibit kinase activity. Further experiments are required to validate this possible regulatory mechanism.

A second example of such regulation is the 14-3-3 phosphobinding domain family. The highly specific enrichment of ubiquitylation in the phosphobinding region suggests that ubiquitylation can be used to inhibit 14-3-3 interaction with its targets. Inhibition of dimerization is plausible, given the enrichment of ubiquitylation in the dimerization region. It is likely that ubiquitin functions to reversibly regulate 14-3-3 activity; however, the nature of this regulation remains unclear.

PTM cross-talk is a complex and multifaceted landscape that is largely unexplored. New proteomics technologies, such as we describe here, now offer a practical approach to characterize modification cross-talk and to elucidate its complexity and influence.

METHODS

Methods and any associated references are available in the online version of the paper.

Note: Supplementary information is available in the online version of the paper.

ACKNOWLEDGMENTS

We acknowledge J. Hsu for experimental assistance, R.A. Rodriguez-Mias for helpful discussions, and members of the Villén lab for critical reading of the manuscript. This work is supported in part by US National Institutes of Health (NIH) grants R00CA140789 (to J.V.) and P50 GM082250, P01 AI090935, P50 GM081879 and P01 AI091575 (to N.J.K.). S.F. is supported by the Howard Hughes Medical Institute.

AUTHOR CONTRIBUTIONS

D.L.S. and J.V. designed research. D.L.S. and L.S. performed research. D.L.S. and P.B. analyzed data. S.F., N.J.K. and J.V. supervised research. A.G. and J.R. provided reagents. D.L.S., P.B. and J.V. wrote the paper. All authors discussed the results and edited the manuscript.

COMPETING FINANCIAL INTERESTS

The authors declare competing financial interests: details are available in the online version of the paper.

1. Jenuwein, T. & Allis, C.D. Translating the histone code. *Science* **293**, 1074–1080 (2001).
2. Hunter, T. The age of crosstalk: phosphorylation, ubiquitination, and beyond. *Mol. Cell* **28**, 730–738 (2007).
3. Ichimura, T. *et al.* 14-3-3 proteins modulate the expression of epithelial Na^+ channels by phosphorylation-dependent interaction with Nedd4-2 ubiquitin ligase. *J. Biol. Chem.* **280**, 13187–13194 (2005).
4. Khosravi, R. *et al.* Rapid ATM-dependent phosphorylation of MDM2 precedes p53 accumulation in response to DNA damage. *Proc. Natl. Acad. Sci. USA* **96**, 14973–14977 (1999).
5. Emanuele, M.J. *et al.* Global identification of modular cullin-RING ligase substrates. *Cell* **147**, 459–474 (2011).
6. Kim, W. *et al.* Systematic and quantitative assessment of the ubiquitin-modified proteome. *Mol. Cell* **44**, 325–340 (2011).
7. Wagner, S.A. *et al.* A proteome-wide, quantitative survey of *in vivo* ubiquitylation sites reveals widespread regulatory roles. *Mol. Cell Proteomics* **10**, M111.013284 (2011).
8. Olsen, J.V. *et al.* Quantitative phosphoproteomics reveals widespread full phosphorylation site occupancy during mitosis. *Sci. Signal.* **3**, ra3 (2010).
9. Huttlin, E.L. *et al.* A tissue-specific atlas of mouse protein phosphorylation and expression. *Cell* **143**, 1174–1189 (2010).
10. van Noort, V. *et al.* Cross-talk between phosphorylation and lysine acetylation in a genome-reduced bacterium. *Mol. Syst. Biol.* **8**, 571 (2012).
11. Yao, Q., Li, H., Liu, B.Q., Huang, X.Y. & Guo, L. SUMOylation-regulated protein phosphorylation, evidence from quantitative phosphoproteomics analyses. *J. Biol. Chem.* **286**, 27342–27349 (2011).
12. Beltrao, P. *et al.* Systematic functional prioritization of protein posttranslational modifications. *Cell* **150**, 413–425 (2012).
13. Peng, J. *et al.* A proteomics approach to understanding protein ubiquitination. *Nat. Biotechnol.* **21**, 921–926 (2003).
14. Beausoleil, S.A. *et al.* Large-scale characterization of HeLa cell nuclear phosphoproteins. *Proc. Natl. Acad. Sci. USA* **101**, 12130–12135 (2004).
15. Gauci, S. *et al.* Lys-N and trypsin cover complementary parts of the phosphoproteome in a refined SCX-based approach. *Anal. Chem.* **81**, 4493–4501 (2009).
16. Nguyen Ba, A.N. & Moses, A.M. Evolution of characterized phosphorylation sites in budding yeast. *Mol. Biol. Evol.* **27**, 2027–2037 (2010).
17. Landry, C.R., Levy, E.D. & Michnick, S.W. Weak functional constraints on phosphoproteomes. *Trends Genet.* **25**, 193–197 (2009).
18. Kõivomägi, M. *et al.* Cascades of multisite phosphorylation control Sic1 destruction at the onset of S phase. *Nature* **480**, 128–131 (2011).
19. Nash, P. *et al.* Multisite phosphorylation of a CDK inhibitor sets a threshold for the onset of DNA replication. *Nature* **414**, 514–521 (2001).
20. Henchoz, S. *et al.* Phosphorylation- and ubiquitin-dependent degradation of the cyclin-dependent kinase inhibitor Far1p in budding yeast. *Genes Dev.* **11**, 3046–3060 (1997).
21. Sia, R.A.L., Bardes, E.S.G. & Lew, D.J. Control of Swe1p degradation by the morphogenesis checkpoint. *EMBO J.* **17**, 6678–6688 (1998).
22. Belle, A. Quantification of protein half-lives in the budding yeast proteome. *Proc. Natl. Acad. Sci. USA* **103**, 13004–13009 (2006).
23. Liu, Q. *et al.* SCF^{Cdc4} enables mating type switching in yeast by cyclin-dependent kinase-mediated elimination of the Ash1 transcriptional repressor. *Mol. Cell Biol.* **31**, 584–598 (2011).
24. Kaplun, L., Ivantsiv, Y., Bakhrat, A. & Raveh, D. DNA damage response-mediated degradation of Ho endonuclease via the ubiquitin system involves its nuclear export. *J. Biol. Chem.* **278**, 48727–48734 (2003).
25. Kishi, T., Ikeda, A., Koyama, N., Fukada, J. & Nagao, R. A refined two-hybrid system reveals that SCFCdc4-dependent degradation of Swi5 contributes to the regulatory mechanism of S-phase entry. *Proc. Natl. Acad. Sci. USA* **105**, 14497–14502 (2008).
26. Tebb, G., Moll, T., Dowzer, C. & Nasmyth, K. SWI5 instability may be necessary but is not sufficient for asymmetric HO expression in yeast. *Genes Dev.* **7**, 517–528 (1993).
27. Jaquenoud, M., Gulli, M.P., Peter, K. & Peter, M. The Cdc42p effector Gic2p is targeted for ubiquitin-dependent degradation by the SCF^{Grr1} complex. *EMBO J.* **17**, 5360–5373 (1998).
28. Chevalier, D., Morris, E.R. & Walker, J.C. 14-3-3 and FHA domains mediate phosphoprotein interactions. *Annu. Rev. Plant Biol.* **60**, 67–91 (2009).
29. Narayanan, A. & Jacobson, M.P. Computational studies of protein regulation by post-translational phosphorylation. *Curr. Opin. Struct. Biol.* **19**, 156–163 (2009).

ONLINE METHODS

Yeast culture. For proteomic experiments, the following strain was used: *S. cerevisiae* LSY207 (*MATa lys2-801*, *ura3-52*, *leu2-3,112*, *his3Δ200*, *trp1-1*, *ubi1ΔTRP1*, *ubi2Δura3*, *ubi3Δ*, *ubi4ΔLEU2*, *pdr5::KanMX* [pUB221] [pUB100]). pUB221 is a *URA3*-marked plasmid that expresses 6His-*myc*-ubiquitin under a *CUP1* promoter, whereas pUB100 expresses the essential ribosomal protein encoded by the *ubi1* gene[3,4,30,31]. LSY207 was grown in lysine-free synthetic complete medium supplemented with either 436 μM light lysine (K0) or heavy lysine (K8). For qualitative experiments 1 liter of cells were grown in K0 medium. For proteasome inhibition experiments, two 1-liter cultures were grown. The control culture was grown in K0 medium, to which 1.54 mL of DMSO was added 1 h before harvesting[18,19,21,32,33]. The other culture was grown in K8 medium and was exposed to 50 μM bortezomib in DMSO (1.54 mL) 1 h before harvesting (LC Laboratories). All cultures were harvested during mid-log phase ($OD_{600} \approx 1.0$).

Sample preparation. All steps were performed at 4 °C unless otherwise noted. Harvested cells were washed with water and resuspended in 8-10 mL of lysis buffer containing 8 M urea, 300 mM NaCl, 50 mM Tris, pH 8.2, 50 mM NaF, 50 mM Na-β-glycerophosphate, 10 mM Na-pyrophosphate, 1 mM Na-orthovanadate and 1 tablet of mini protease inhibitor (Roche). For SILAC experiments, cells were mixed 1:1. Cell suspensions were transferred to 2-mL screw-cap tubes and lysed by four repetitions of bead beating (1 min beating, 1.5 min rest). Tubes were spun first at 100*g* to remove beads and subsequently at 10,000*g* to pellet cellular debris. The supernatants were pooled. At this point, 10% of the sample was removed for SCX-IP experiments (~9–20 mg protein).

The remaining sample was transferred to a tube containing 2.5 mL of equilibrated cobalt-NTA resin (Talon Superflow Resin; Clontech Laboratories) and incubated for 40 min at 4 °C to affinity-purify ubiquitylated proteins via the His tag. The flow-through was further depleted of ubiquitin-containing proteins by two subsequent incubations with fresh cobalt resin. The ubiquitin-containing proteins bound to the resin were washed twice with 8 mL of equilibration buffer (8 M urea, 300 mM NaCl, 50 mM Tris, pH 8.2) and twice with equilibration buffer supplemented with 10 mM imidazole. Finally, ubiquitin containing proteins were eluted with 7 mL of equilibration buffer containing 150 mM imidazole followed by 1.5 mL of equilibration buffer containing 300 mM imidazole.

Proteins were reduced in 5 mM DTT for 45 min at RT and alkylated with 15 mM iodoacetamide for 45 min at RT in the dark. Alkylation was capped by incubation with 15 mM DTT at RT for 15 min.

The qualitative experiment resulted in three aliquots: (i) for SCX-IP purification, (ii) ubiquitin-enriched proteins eluted from the cobalt resin ('ubiquitylated proteins') and (iii) ubiquitin-depleted proteins that did not bind to the cobalt resin ('nonubiquitylated proteins'). Each of these aliquots were diluted 4.5-fold with 50 mM Tris, pH 8.2, and digested overnight at 37 °C with 100 μg of trypsin (Promega).

In the proteasome inhibition experiment we used the same three aliquots as described above for the qualitative experiments; however, the digestion schema was different to ensure that all peptides contained a lysine residue required for peptide quantification. In this case, the ubiquitin-enriched and ubiquitin-depleted aliquots were diluted twofold with 50 mM Tris, pH 8.9, and 80 μg or 240 μg of lysyl endopeptidase (LysC) were added, respectively (Wako). After 4 h of incubation at RT, half of the ubiquitin-enriched sample was removed; this was used for phosphopeptide enrichment. The remaining half of this aliquot and the sample for SCX-IP were both to be enriched for diGly-containing peptides (see "Immunoprecipitation of diGly-containing peptides"). Thus, they were diluted to 1.8 M urea with 50 mM Tris, pH 8.2, and digested with 100 μg trypsin overnight at 37 °C (Promega). After enzymatic digestion, all samples were acidified to ~2 pH with TFA and desalted on tC18 Sep-Pak cartridges (Waters).

SCX-based peptide fractionation. Peptides not subjected to His-tag purification (i.e., SCX-IP samples) were fractionated over a Polysulfoethyl A SCX cartridge (PolyLC)[2,34]. Two buffers were used to fractionate the peptides: (A) 5 mM KH_2PO_4, 30% acetonitrile, pH 2.65, and (B) 5 mM KH_2PO_4, 350 mM KCl, 30% acetonitrile, pH 2.65. Cartridges were first conditioned with a decreasing percentage of SCX buffer B, which was followed by equilibration in SCX buffer A. Samples dissolved in SCX buffer A were loaded onto the cartridge, and peptides were stepwise eluted with increasing concentration of salt (0%, 15%, 18%, 21%, 24%, 27% and 80% buffer B). Eluents were lyophilized and then desalted on tC18 Sep-Pak cartridges before enrichment of diGly-containing peptides via immunoprecipitation. This method was used to enrich for peptides concurrently modified with phosphorylation and diGly.

Nonubiquitylated peptide samples were separated into 12 fractions via column-based SCX. For qualitative experiments, 2 mg of peptides were separated on a 4.6 mm × 200 mm Polysulfoethyl A (5-μm, 300-Å) column, whereas for SILAC experiments, 10 mg of peptides were separated on a 9.4 mm × 200 mm column. The gradient conditions were essentially as described elsewhere[8,9,34,35]. All fractions were dried and desalted on tC18 Sep-Pak cartridges before phosphopeptide enrichment. A separate aliquot of 1 mg of ubiquitin-depleted sample was also fractionated on a 30-mg Oasis cartridge (Waters) by reverse phase at basic pH. The cartridge was conditioned with 80% acetonitrile in 20 mM ammonium hydroxide and equilibrated with 20 mM ammonium hydroxide. The sample was loaded in 1 mL of water, and stepwise elution of peptides was achieved by increasing acetonitrile concentration in 20 mM ammonium hydroxide (0%, 6%, 9%, 12%, 15%, 18%, 30% and 80% acetonitrile elutions). A 10-μg aliquot of the ubiquitin-enriched LysC digest was also fractionated in this manner on an Empore C18 stage tip (3M), except elutions at 15% and 30% acetonitrile were omitted[5–7,36]. This sample was used to acquire protein quantification on ubiquitylated proteins.

Immunoprecipitation of diGly-containing peptides. Peptide immunoprecipitations were performed essentially as described elsewhere[10,11,37]. Samples were dissolved in 1.4 mL of IAP buffer (50 mM MOPS-NaOH, pH 7.2, 10 mM Na_2HPO_4, 50 mM NaCl) and spun at 4 °C for 10 min at 4,000*g*. For each sample, 80 μg of diGly antibody loaded on protein A agarose beads was used (Cell Signaling Technology)[6,13]. The antibody was first washed twice with PBS and then washed three times with IAP. The supernatants of the samples were then incubated with the antibody at 4 °C for 40 min with gentle rotation. The antibody was then washed three

times with IAP and twice with water. The antibody was incubated for 10 min in 100 µL of 0.15% TFA to elute diGly peptides. This elution was repeated two more times, and all elutions were pooled and desalted on stage tips[14,15,36].

The flow-through of the diGly immunoprecipitations of the SCX-IP samples were each desalted on 100-mg tC18 Sep-Pak cartridges, and an aliquot of this was analyzed via MS.

Phosphopeptide enrichment. Both the ubiquitin-enriched LysC digested sample (SILAC experiment) and the flow-through of the qualitative ubiquitin-enriched trypsin diGly IP peptide mixtures were enriched for phosphopeptides using 150 µL of magnetic NTA-IMAC beads (Qiagen)[13,30,38]. Phosphopeptide enrichment was also performed on the peptides from the ubiquitin-depleted sample fractionated via SCX. Here 300 µL of magnetic NTA-IMAC beads were used in total. The beads were washed three times with water and then incubated with 40 mM EDTA, pH 8, for 30 min. Next the beads were washed three times with water and then incubated with 100 mM $FeCl_3$ for 30 min. The beads were then washed with 80% acetonitrile, 0.1% TFA three times. Samples were dissolved in either 150 µL (fractions) or 300 µL (diGly IP flow-through) and incubated with the IMAC beads for 30 min with agitation. The beads were then washed three times with 80% acetonitrile, 0.1% TFA, and the phosphopeptides were eluted with 100 µL of 50% acetonitrile, 25% ammonium hydroxide. The eluent was quickly passed through a stage tip to filter out any beads and immediately acidified to a pH of ~3 with formic acid. The eluent was then dried and resuspended in 4% formic acid, 3% acetonitrile for MS analysis.

Mass spectrometry analysis. Peptides were resuspended in 4% formic acid, 3% acetonitrile and loaded onto a 100-µm ID × 3-cm precolumn packed with Maccel C18 3-µm, 200-Å particles (The Nest Group) for nRPLC-MS/MS analysis in a Velos Orbitrap mass spectrometer (Thermo Fisher). Peptides were eluted over a 75-µm ID × 26-cm analytical column packed with the same material. The exact gradient conditions were tailored to the complexity and chemical properties of each sample; however, generally the gradient was 8–30% acetonitrile in 0.15% formic acid over the course of 90 or 120 min. All MS spectra were collected with Orbitrap detection. Two types of MS/MS spectra were collected: either resonant-excitation collision-activated dissociation with ion-trap detection (CAD) or beam-type collision-activation dissociation (HCD) with Orbitrap detection. Nonmodified peptide samples were analyzed by CAD, whereas modified peptides samples were independently analyzed by both HCD and CAD. When MS/MS spectra were collected in the linear ion trap, the 20 most abundant ions were selected in a data-dependent manner, whereas for MS/MS collected in the Orbitrap, the ten most abundant ions were selected. The exact mass spectrometer settings can be found in the RAW files provided at http://faculty.washington.edu/jvillen/lab/.

Identification and quantification of peptides, proteins and modifications. MS/MS spectra were searched with Sequest[10,39] against the SGD yeast proteome (downloaded 5 January 2011). The precursor mass tolerance was set to 50 p.p.m., and the fragment-ion tolerance was set to 0.36 Da with a 0.11-Da offset. A static modification on cysteine residues (57.021464 Da) and a variable modification of methionine oxidation (15.994914 Da) were used for all searches. For non-SILAC experiments, additional variable modifications representing phosphorylation of serine, threonine or tyrosine (79.966333 Da) or diGly on lysine (114.042928 Da) were used where appropriate. For SILAC experiments, an additional variable modification of heavy lysine (8.014198 Da) was considered. Search results were filtered to a 1% FDR at the peptide and protein level according to experimental group (i.e., ubiquitin enriched, depleted or SCX-IP)[18–21,40]. Phosphorylation and ubiquitylation sites were localized using an in-house implementation of the Ascore algorithm[41]. Sites with an Ascore >13 ($P < 0.05$) were considered confidently localized, and diGly modifications localized to the C-terminal peptide residue were discarded. For non-SILAC experiments, only confidently localized modification sites were reported. For SILAC experiments, modification isoforms—rather than single sites—were listed. Only those proteins that were identified as containing a diGly modification were considered ubiquitylated. For SCX-IP experiments, phosphorylation sites on ubiquitylated proteins were considered to be only those found on the same peptide as a diGly modification. From the His-tag elution experiments, phosphorylation sites reported were restricted to those identified on proteins for which a diGly modification was also identified.

Peptides were quantified using in-house software measuring chromatographic peak maximum intensities. Only peptides with a summed SNR of the light and heavy peptide >7 were considered. The peak maxima for peptides with the same combination of modification sites were summed before calculating a ratio. When modification sites could not be localized, the region of amino acids the site could reside in was listed. Proteins were quantified by first summing maximum peak intensities of all unmodified peptides for a given protein. The ratio was calculated between the sum of all peptides for a protein from heavy-labeled cells and the sum from light-labeled cells. In instances in which only the light or heavy form was identified, the noise signal level was used as the signal of the missing peptide. Abundance ratios for both modification sites and proteins were all normalized by the same magnitude to adjust for mixing errors. This normalization adjusted the distribution of protein quantitative ratios such that the median was set to $\log_2 = 0$. Co-regulated phosphorylation and ubiquitylation was defined as pair of modification site isoforms that had either (i) a minimum abundance change of ~60% for each, with the magnitude of change for one isoform within 15% of the other, or (ii) a minimum abundance change of 100% (twofold) for both.

Site mutagenesis and western blotting. Plasmids encoding HA-tagged proteins (Open Biosystems yeast ORF collection) were purified and subjected to site-directed mutagenesis[6,42]. Wild-type amino acids were either converted to alanine (to represent a non-phosphorylated state) or glutamic acid (to represent a phosphorylated state). The wild-type and Swi5 T323A mutant plasmids were introduced into the Y258 strain (*MATa his4-580*, *ura3-52*, *leu2-3,112*, *pep4-3*), and the Swi5 WT and Swi5 T323E mutant plasmid were introduced into a Y258 strain carrying a *PDR5* deletion (*MATa his4-580*, *ura3-52*, *leu2-3,112*, *pep4-3*, *pdr5::KanMX*). Overexpression of the plasmid was induced with galactose incubation (4–6 h). For Swi5 T323A and Swi5 WT, cycloheximide was added to inhibit translation (50 µg/mL), and 2 mL of cell

doi:10.1038/nmeth.2519

culture was harvested after 0, 20 and 40 min. For Swi5 WT and Swi5 T323E, bortezomib was added to inhibit the proteasome (100 μM), and 1.5 mL of cell culture was harvested after 0, 30, 60 and 90 min. Additional strains containing mutants in the Gic2 protein were generated from GST-tagged proteins (Open Biosystems yeast GST collection), and cycloheximide degradation assays were performed exactly as described above for Swi5. For Gic2, WT protein expression was observed to be higher than that of either mutant; therefore, mutant strains were induced for 4 h, whereas the WT strain was induced for 30 min. This produced similar protein expression for the mutant and WT forms. Harvested cells were lysed by bead beating in 50 mM Tris, pH 8.2, 1 mM EDTA, 0.5% Triton X-100, 100 mM NaCl, 1 mM DTT and 1 tablet mini protease inhibitor (Roche). LDS denaturing buffer was added (1×), and samples were incubated at 100 °C for 5 min. Clarified cell lysates were separated by SDS-PAGE followed by immunoblotting with the anti HA-tag antibody (0.33 μg/mL, GenScript #A01244), anti-GST antibody (0.25 μg/mL, GenScript #A000865) or anti–α-tubulin (loading control, 0.17 μg/mL, GenScript #A01410). Western blot images were processed and quantified using the freely available ImageJ software (http://rsbweb.nih.gov/ij/index.html).

Bioinformatics: conservation, functional enrichment and structural analysis. Protein sequence alignments between yeast, human and mouse were done with MUSCLE version 3.6 using standard alignments options[22,43]. Human and mouse PTMs were obtained from PhosphoSitePlus (http://www.phosphosite.org/)[44]. To avoid potential redundancies and issues with gene duplication, we used only putative 1-to-1 orthologs as predicted with 90% confidence by the InParanoid algorithm (orthology information available at http://inparanoid.sbc.su.se/)[45]. To account for errors in the PTM positional assignments, we defined a PTM site to be conserved if the aligned peptide of the ortholog protein is also known to be modified within a window of ±2 alignment positions. To estimate a random expectation (i.e., null model) for the conservation of PTM sites from species A to species B, we randomly shuffled the PTM sites of each protein in species A. The random shuffling was done only from possible acceptor residues (K for ubiquitylation and S/T for phosphorylation). We excluded tyrosine acceptor residues from the sampling, as these constitute a minority of phosphosites. The ratios of conserved over expected values for the different groups of PTMs were compared using a Mann-Whitney ranked test.

Gene ontology enrichment analysis was performed using Babelomics4 (http://babelomics.bioinfo.cipf.es/), and *P* values were calculated using a two-tailed Fisher exact test with correction for multiple testing[46]. For assessment of differences in protein half-lives, a two-tailed Wilcoxon test was performed.

To search for significant enrichment of PTMs within specific regions of domain families, we selected for each domain a representative structure and transferred the PTMs, occurring in all instances of this domain in different species (mouse, human and the yeast *S. cerevisiae*), using protein sequence alignments[5–7]. We then used a sliding window of ten amino acids and random sampling to identify regions, within each domain family, that were enriched for PTMs. Any ten amino-acid peptide with a significant ($P < 0.005$) enrichment of PTMs when compared to random was defined a potential regulatory region[12].

Three known phosphodegron motifs (or protein sequence patterns) were obtained from the ELM database (http://elm.eu.org/). The three patterns used were [LIVMP]X{0,2}[ST]PXX[ST] or [LIVMP]X{0,2}[ST]PXXE or [ST]GX{1,3}[ST]. X represents any amino acid, square brackets represent a position that accepts any of the amino acids within brackets, and curly brackets describe the number of times that the preceding amino acid can be repeated. As an example, X{0,2} means that 0–2 random amino acids can fit this position(s).

For analysis of modification-site protein structural proximity, we obtained yeast homology models from ModBase database (http://modbase.compbio.ucsf.edu/) and calculated the spatial distance (i.e., angstroms between α carbons) between modification sites[47].

30. Starita, L.M., Lo, R.S., Eng, J.K., von Haller, P.D. & Fields, S. Sites of ubiquitin attachment in *Saccharomyces cerevisiae*. *Proteomics* **12**, 236–240 (2012).
31. Spence, J. *et al.* Cell cycle–regulated modification of the ribosome by a variant multiubiquitin chain. *Cell* **102**, 67–76 (2000).
32. Zhu, H., Pan, S., Gu, S., Bradbury, E.M. & Chen, X. Amino acid residue specific stable isotope labeling for quantitative proteomics. *Rapid Commun. Mass Spectrom.* **16**, 2115–2123 (2002).
33. Ong, S.-E. Stable isotope labeling by amino acids in cell culture, SILAC, as a simple and accurate approach to expression proteomics. *Mol. Cell Proteomics* **1**, 376–386 (2002).
34. Villén, J., Beausoleil, S.A., Gerber, S.A. & Gygi, S.P. Large-scale phosphorylation analysis of mouse liver. *Proc. Natl. Acad. Sci. USA* **104**, 1488–1493 (2007).
35. Villén, J. & Gygi, S.P. The SCX/IMAC enrichment approach for global phosphorylation analysis by mass spectrometry. *Nat. Protoc.* **3**, 1630–1638 (2008).
36. Rappsilber, J., Ishihama, Y. & Mann, M. Stop and go extraction tips for matrix-assisted laser desorption/ionization, nanoelectrospray, and LC/MS sample pretreatment in proteomics. *Anal. Chem.* **75**, 663–670 (2003).
37. Rush, J. *et al.* Immunoaffinity profiling of tyrosine phosphorylation in cancer cells. *Nat. Biotechnol.* **23**, 94–101 (2005).
38. Ficarro, S.B. *et al.* Magnetic bead processor for rapid evaluation and optimization of parameters for phosphopeptide enrichment. *Anal. Chem.* **81**, 4566–4575 (2009).
39. Eng, J.K., McCormack, A.L. & Yates, J.R. III. An approach to correlate tandem mass spectral data of peptides with amino acid sequences in a protein database. *J. Am. Soc. Mass Spectrom.* **5**, 976–989 (1994).
40. Elias, J.E. & Gygi, S.P. Target-decoy search strategy for increased confidence in large-scale protein identifications by mass spectrometry. *Nat. Methods* **4**, 207–214 (2007).
41. Beausoleil, S.A., Villén, J., Gerber, S.A., Rush, J. & Gygi, S.P. A probability-based approach for high-throughput protein phosphorylation analysis and site localization. *Nat. Biotechnol.* **24**, 1285–1292 (2006).
42. Gelperin, D.M. *et al.* Biochemical and genetic analysis of the yeast proteome with a movable ORF collection. *Genes Dev.* **19**, 2816–2826 (2005).
43. Edgar, R.C. MUSCLE: multiple sequence alignment with high accuracy and high throughput. *Nucleic Acids Res.* **32**, 1792–1797 (2004).
44. Hornbeck, P.V. *et al.* PhosphoSitePlus: a comprehensive resource for investigating the structure and function of experimentally determined post-translational modifications in man and mouse. *Nucleic Acids Res.* **40**, D261–D270 (2012).
45. O'Brien, K.P., Remm, M. & Sonnhammer, E.L. Inparanoid: a comprehensive database of eukaryotic orthologs. *Nucleic Acids Res.* **33**, D476–D480 (2005).
46. Medina, I. *et al.* Babelomics: an integrative platform for the analysis of transcriptomics, proteomics and genomic data with advanced functional profiling. *Nucleic Acids Res.* **38**, W210–W213 (2010).
47. Pieper, U. *et. al.* MODBASE, a database of annotated comparative protein structure models, and associated resources. *Nucleic Acids Res.* **32**, D217–D222 (2004).